NOAA ROSES Semi-Annual Report

Reporting Period: March 2021 – August 2021 (2nd report)

PI: Jim Jung
Co-PI(s): Agnes Lim, Zhenglong Li

Project Title: Assimilation of radiance tendency of water vapor bands from geostationary satellites using FV3GFS

Executive Summary (1 paragraph max)

The objective of this project is to investigate a new approach for assimilating radiance tendency water vapor observations. These observations are available from the advanced imagers onboard domestic and international geostationary satellites, such as Advanced Baseline Imager (ABI) on the Geostationary Operational Environmental Satellite-R (GOES-R) series, Advanced Himawari Imager on Himiwari-8/9, and Advanced Meteorological Imager on Geostationary - Korea Multi-Purpose Satellite-2. The advantage of assimilating radiance tendency is that it does not require a bias correction, because the radiance tendencies from both observations and background can be considered bias free within a short period of time (i.e. 6 hours). The bias correction, used to remove biases between observations and background for traditional assimilation technique, may reduce or compromise the useful information in the observations. The proposed work will develop the technical methodology, test and assess the impact of radiance tendency assimilation from domestic and international geostationary satellites on global weather forecast skill using a recent version of the Finite-Volume Cubed-Sphere dynamical core Global Forecast System (FV3GFS) that has a 4-D hybrid Ensemble Variational data assimilation system.

Progress toward FY20 Milestones and Relevant Findings (with any Figs)

1. The technique to allow radiance tendency assimilation was developed and implemented in FV3GFS. This includes code changes to read in radiance tendency for the three Advanced Baseline Imager (ABI) water vapor bands. Tools have been developed to calculate the radiance tendency from the ABI Clear Sky Radiance product. For radiance tendency assimilation, the cost function is revised as $\boldsymbol{J}(\boldsymbol{x}) = \left(\boldsymbol{x}-\boldsymbol{x}^{\boldsymbol{b}}\right)^{\boldsymbol{T}}\boldsymbol{B}^{-\mathbf{1}}\left(\boldsymbol{x}-\boldsymbol{x}^{\boldsymbol{b}}\right) + [\boldsymbol{y}^{\boldsymbol{ART}}-\boldsymbol{H}(\boldsymbol{x})]^{\boldsymbol{T}}\boldsymbol{R}^{-\mathbf{1}}[\boldsymbol{y}^{\boldsymbol{ART}}-\boldsymbol{H}(\boldsymbol{x})]$, where $\boldsymbol{x}$ is the state variable, $\boldsymbol{x}^{\boldsymbol{b}}$ is the background, $\boldsymbol{B}$ is the background error covariance matrix, the superscript $\boldsymbol{T}$ denotes transpose, $\boldsymbol{y}^{\boldsymbol{ART}}$ is the modified new observation for radiance tendency assimilation (***ART*** stands for assimilating radiance tendency), $\boldsymbol{H}(\boldsymbol{x})$ is the simulated radiances from the background, and $\boldsymbol{R}$ is the observation error covariance matrix. The modified new observation is calculated based on $\boldsymbol{y}^{\boldsymbol{ART}} = \boldsymbol{y}-\boldsymbol{y}_{\mathbf{0}}+\boldsymbol{H}\left(\boldsymbol{x}_{\mathbf{0}}\right)$, where $\boldsymbol{y}$ is the observed radiance at current time step, $\boldsymbol{y}_{\mathbf{0}}$ is the observed radiance at previous time step, $\boldsymbol{y}-\boldsymbol{y}_{\mathbf{0}}$ is the radiance tendency observation, $\boldsymbol{H}\left(\boldsymbol{x}_{\mathbf{0}}\right)$ is the simulated radiances from the background at previous time step. This form of the cost function makes it easier to implement the technique of radiance tendency assimilation. There are two options for the background at previous time step, or $\boldsymbol{x}_{\mathbf{0}}$; (1) the hourly forecast fields from the previous analysis such that radiance tendency is the difference between two observations at the same location separated by 1 hour and (2) analysis

from the last cycle. In option 2, the radiance tendency is the difference between observation time and the previous analysis time. In the second half of the fiscal year, Option 1 was implemented. Option 2 will be implemented and tested later. Two experiments were conducted. The first experiment used the default observation error covariance matrix (***1R***), i.e., the same as the control run. And the second used half of the default observation error covariance matrix (***0.5R***). The results were compared with the control run to check the implementation of the technique for radiance tendency assimilation. Figure 1 shows the time series of the mean and standard deviation of observation-background (O-B) and observation-analysis (O-A) for the three experiments. The control run has bias correction. The two radiance tendency assimilation experiments have no bias correction. Findings include:

a) The control run is effective in assimilating the ABI water vapor band radiances. The standard deviations are reduced by more than 0.2 K for all time steps and all three bands. The mean bias of all three bands at all time steps is reduced as well.

b) The radiance tendency assimilation with the default observation error covariance matrix (***1R***): reductions in standard deviations are not obvious for band 8, but become more substantial for bands 9 and 10. If zoom-in to bands 9 and 10 of the standard deviation panels (right two panels in the bottom row in Figure 1), the green solid line is below the dashed line. However, the overall change from O-B to O-A is subtle. Further investigation reveals that standard deviations of analysis-background is much smaller for radiance tendency assimilation than the control run, possibly suggesting that the assimilation of radiance tendency has not efficiently exploited the information in the radiance tendency. This could possibly be due to the large error assigned in the observation error covariance matrix; 3K for band 8, 2.5K for band 9 and 2K for band 10. Additional experiment was carried out to investigate the impact of the observation error covariance matrix on radiance tendency assimilation.

c) The radiance tendency assimilation with half of the default observation error covariance matrix (***0.5R***): improved standard deviation reductions for all time steps and all three WV bands are seen. For all three bands, the standard deviation (bottom row in Figure 1) of O-A (blue solid lines) are smaller than O-B (blue dashed lines). This indicates larger observation weights help. In the control run, the observation error covariance matrix is a sum of the contributions from observation, background, forward models, and representative errors. In radiance tendency assimilation, the last three components are greatly reduced from the time differencing. The observation error of the radiance tendency itself, on the other hand, is increased by 41%. The calibration of ABI/GOES-16 shows that all three water vapor bands have the noise equivalent differential temperature less than 0.08K at 240K. So the observation error covariance matrix of radiance tendency may be further reduced. Additional experiments will be carried out to test a quarter (***0.25R***) and one eighth (***0.125R***) of the default observation error covariance matrix. The purpose is to understand the impact of the observation error covariance matrix on ABI radiance tendency assimilation and possibly to find the optimal one. There is no significant change in the number of observations assimilated when different observation error covariance matrix is used.

d) The mean biases of O-B and O-A for radiance tendency assimilation are similar between different experiments. This is probably because the mean bias of radiance tendency is already very small to begin with. Note that there is no bias correction in radiance tendency assimilation. This supports the assumption of the radiance tendency assimilation that the radiance biases do not change dramatically within a short period of time, whether they are from observation, or background.

2. In first half of the fiscal year, a machine learning based quality control scheme for surface contamination is developed and applied to three ABI water vapor radiances. The advantage of this technique is that it is objective because it relies on observations only. Impact studies on Hurricane Harvey (2017) were carried out in this second half of the fiscal year with the Weather Research and Forecasting model and the community Gridpoint Statistical Interpolation system. Based on different thresholds used in the quality control scheme, each ABI water vapor radiance is provided with a quality flag category ranging from 1 to 4. Higher number indicates strict threshold used, thus more confidence in the quality controlled data. Numerical experiments were used to find the optimal quality control category for each band based on the Hurricane Harvey (2017) forecast. With the optimal quality control category of each band, Figure 2 shows the mean error and root mean square error (RMSE) of track forecasts are improved when additional bands are added. When band 9 with quality control category 3 is added on top of band 8 (also with category 3), the RMSE of track forecast error is reduced. The improvements are greater as forecast hour increases. The largest improvement, or the reduction of RMSE at 72-hour forecast is around 32 km, or 11%. Over the course of 72 hours of the forecast, the average improvement of RMSE is around 10 km, or 7%. Similarly, band 10 with quality control category 4 also helps improve the track forecast with both bands 8 and 9 assimilated. The largest RMSE reduction at 72-hour forecast is 43 km, or 17% when band 10 is added, and the average improvement of RMSE over the course of 72 hours is 12 km, or 9%. These results suggest that the assimilation of radiances from each of the three ABI water vapor bands with the machine learning based quality control scheme for surface contamination provides independent added value on Hurricane Harvey (2017) track forecast, and the combination of the three bands has the largest impact.

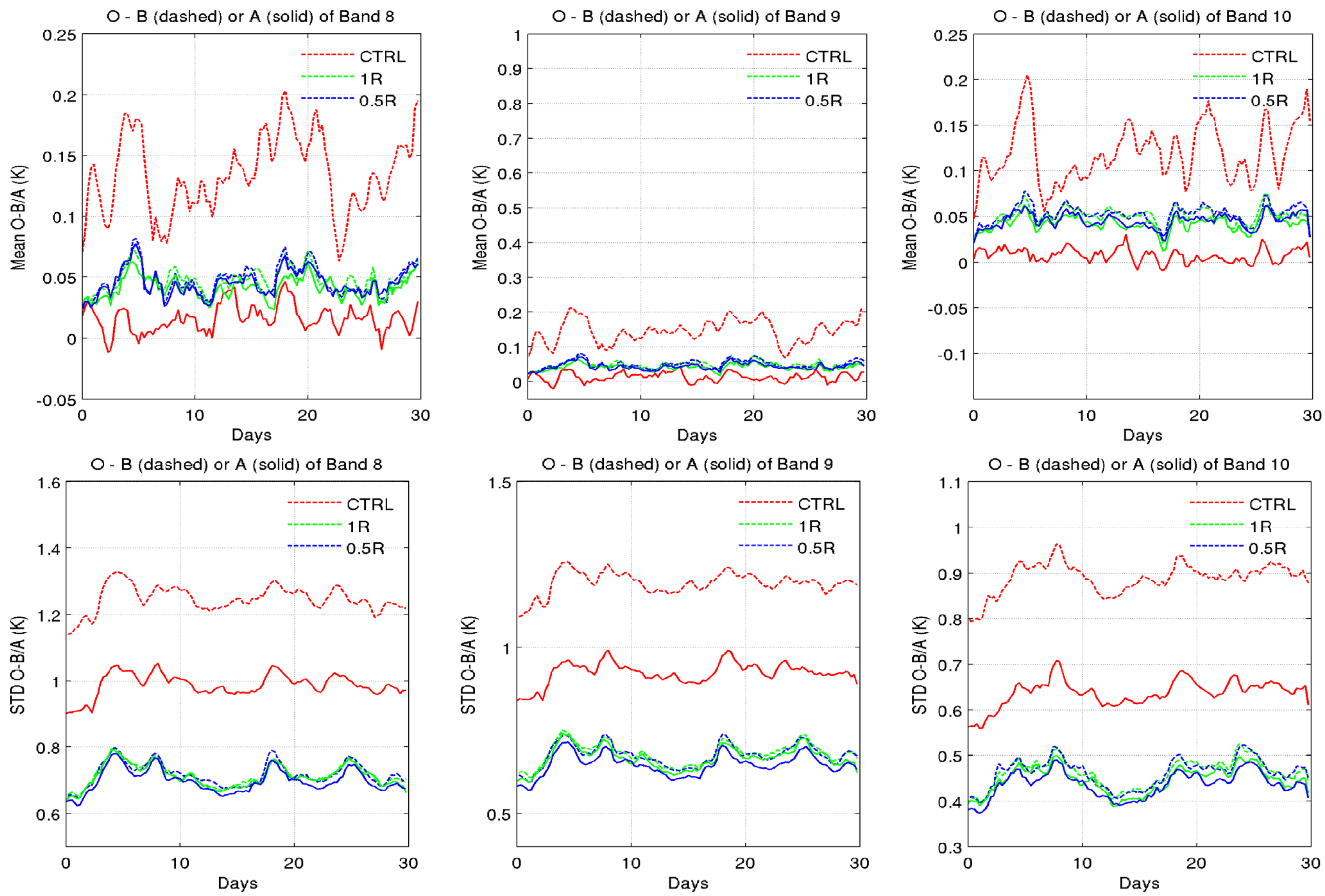

Figure 1. Time series of the mean (top) and the standard deviation (STD, bottom) of observation-background (O-B) and observation-analysis (O-A) from the three experiments: the control run (CTRL, red), the radiance tendency assimilation with Gridpoint Statistical Interpolation default observation error covariance matrix used in the control run (green), and the radiance tendency assimilation with ½ of the default covariance matrix (blue). X-axis shows the days since 00UTC on June 1, 2021. Note that the control run has bias correction while the radiance tendency assimilation has no bias correction.

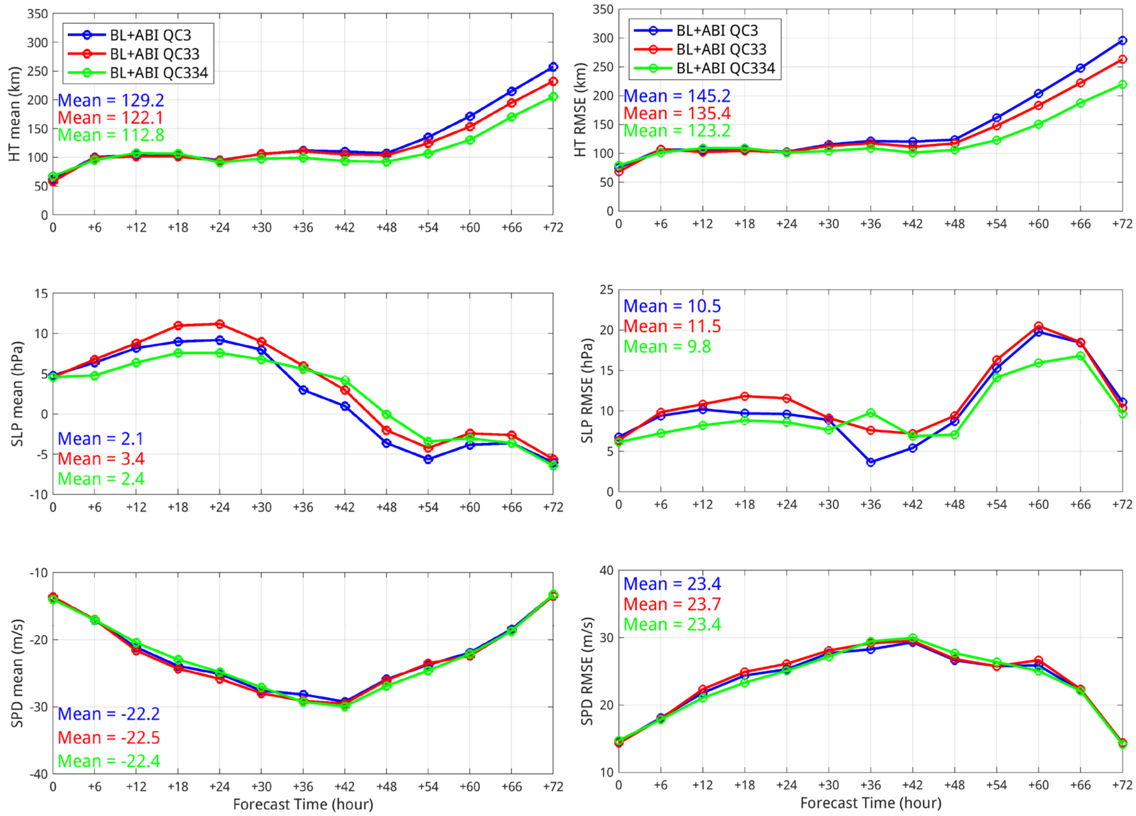

Figure 2. The 72-hour forecast impacts on the mean error (left) and root mean square error (RMSE) (right) of hurricane track (HT, top), minimum seal level pressure (SLP, middle), and maximum wind speed (SPD, bottom) for three different experiments assimilating the baseline measurements plus ABI water vapor radiances from band 8 (blue), bands 8 and 9 (red), and bands 8, 9, and 10 (green). The quality control categories for bands 8, 9, and 10 are 3, 3, and 4 respectively. Note how each of bands 9 and 10 provides additional added value on Hurricane Harvey (2017) track forecast.

Plans for Next Reporting Period

1. Given the improved fits when the observation error covariance matrix is changed from ***1R*** to ***0.5R***, a third experiment with ***0.25R*** will be run, and possibly ***0.125R*** if needed.
2. Forecast impact from experiments with reduced observation error covariance matrix will be assessed.
3. The implementation of radiance tendency assimilation using previous cycle analysis fields (option 2) in FV3GFS will be carried out.
4. The machine learning based surface contamination quality control scheme will be assessed in comparison with existing schemes.